

# Alignment-Dependent Ionization of N<sub>2</sub>, O<sub>2</sub>, and CO<sub>2</sub> in Intense Laser Fields

Simon Petretti, Yulian V. Vanne, and Alejandro Saenz

*AG Moderne Optik, Institut für Physik, Humboldt-Universität zu Berlin, Newtonstr. 15, D-12489 Berlin, Germany*

Alberto Castro

*Instituto de Biocomputación y Física de Sistemas Complejos, Corona de Aragón 42, 50009 Zaragoza, Spain*

Piero Decleva

*Dipartimento di Scienze Chimiche, Università di Trieste, Via L. Giorgieri 1, I-34127 Trieste, Italy*

(Dated: October 30, 2018)

The ionization probability of N<sub>2</sub>, O<sub>2</sub>, and CO<sub>2</sub> in intense laser fields is studied theoretically as a function of the alignment angle by solving the time-dependent Schrödinger equation numerically assuming only the single-active-electron approximation. The results are compared to recent experimental data [D. Pavičić et al., Phys. Rev. Lett. **98**, 243001 (2007)] and good agreement is found for N<sub>2</sub> and O<sub>2</sub>. For CO<sub>2</sub> a possible explanation is provided for the failure of simplified single-active-electron models to reproduce the experimentally observed narrow ionization distribution. It is based on a field-induced coherent core-trapping effect.

Time-resolved imaging of the dynamics of nuclei and electrons on a femtosecond or even sub-femtosecond time scale is a prerequisite for the experimental investigation of the formation and breaking of chemical bonds. Ultrashort laser pulses have recently been demonstrated to allow monitoring of nuclear motion with subfemtosecond and sub-Ångström resolution in real time [1–3]. It was also experimentally demonstrated that the high-harmonic radiation or electrons emitted in an intense laser pulse may in principle reveal electronic structure [4, 5] and thus have the potential for time-resolved imaging of changes of the electronic structure in, e. g., a chemical reaction. To reach this goal it is, however, important to understand the relation between electronic structure and strong-field response in molecules.

In [6] the alignment dependence of the strong-field ionization was measured for N<sub>2</sub>, O<sub>2</sub>, and CO<sub>2</sub>. The found relatively strong angular dependence of the ionization on the incident electric field is interpreted in terms of molecular orbital theory: the measured ionization is supposed to map the structure of the highest occupied molecular orbital (HOMO). While the angle-resolved ionization of N<sub>2</sub> and O<sub>2</sub> reproduces the symmetry of the HOMO and was reasonably explained using a simplified strong-field model like molecular Ammosov-Delone-Krainov (MO-ADK) theory [7], this was not the case for CO<sub>2</sub>.

In order to find out why simple strong-field models like MO-ADK or the molecular strong-field approximation (MO-SFA) [8] fail and are unable to properly reproduce the CO<sub>2</sub> results, a recently introduced approach (SAE-TDSE) to solve the time-dependent Schrödinger equation (TDSE) of a molecule within the single-active-electron approximation (SAE) [9] is adopted in this Letter to calculate the alignment dependence of ionization of N<sub>2</sub>, O<sub>2</sub>, and CO<sub>2</sub>. It avoids most of the assumptions made in the derivations of MO-ADK (a pure tunneling theory) or MO-SFA (that ignores the Coulomb interac-

tion between the emitted electron and the remaining ion) which both neglect excited states. The reliability of the SAE-TDSE has been demonstrated, at least for H<sub>2</sub>, in [9] by a comparison to exact calculations. In this Letter we show that the failure of simple models to explain the experimental CO<sub>2</sub> results in [6] appears to be a laser-induced dynamical coherent coupling of the HOMO and the core, a phenomenon we name *coherent core trapping*.

The SAE-TDSE approach [9] and its present extension to larger molecules and arbitrary orientation is only briefly described here. The basic assumption is that effectively only one single active electron interacts with the external laser field and the corresponding time-dependent Schrödinger equation is then solved numerically. The non-relativistic time-dependent Hamiltonian is treated semi-classically and separated in an unperturbed time-independent molecular part  $H_{\text{mol}}$  and a time-dependent laser-electron interaction  $H_{\text{int}}(t)$ . A fixed molecular geometry is used to calculate the field-free molecular electronic structure which is presently kept invariant during the laser pulse. Experimental values of the equilibrium distances have been adopted in the calculations. The time-dependent wavefunctions are expressed as a linear combination of the solutions of the time-independent field-free Hamiltonian  $H_{\text{mol}}$ . The latter are Kohn-Sham orbitals obtained from density-functional theory using the exchange correlation potential LB94 [10], since it yields the correct asymptotic behavior. The radial parts of the orbitals are expanded in a  $B$ -spline basis consisting of one set that is defined within one large central sphere (with radius  $r_{\text{max}}^0$ ) and additional sets defined within (non-overlapping) atom-centered spheres. While the latter sets assure a proper molecular description of the atomic cores, the former improves the description of molecular bonds and leads to a convenient “box” discretization of the electronic continuum. The angular parts are in both cases expressed in terms of

spherical harmonics and molecular symmetry is fully accounted for. Converged results were obtained for radii  $r_{\max}^0$  200.35 a.u., 160 a.u., and 200.35 a.u. and the values of  $l_{\max}$  10, 12, and 14 for  $\text{N}_2$ ,  $\text{O}_2$ , and  $\text{CO}_2$ , respectively.

In the original SAE scheme (method A) all but a single active electron are frozen in the time propagation. The passive core orbitals are therefore removed from the active space in the TDSE propagation, i.e. the active electron is constrained to remain orthogonal to the *field-free* core. However, all electrons are driven by the field, and due to the unitary evolution under the time-dependent Hamiltonian all orbitals remain orthogonal at all times without the need of external orthogonality constraints. Thus in method B all orbitals are propagated within the complete functional space, including the one occupied by the *field-free* core. Due to the mentioned orthogonality, this does not violate the Pauli principle and insures in fact full gauge invariance of the results, as will be explained elsewhere. Method B may be dubbed independent-active-electron (IAE) approach and is in fact implicit in many model-potential calculations which, however, neglect orthogonality altogether.

The inclusion of symmetries up to  $\Lambda = 6$  where  $\Lambda = 0, 1, 2, \dots$  refers to  $\sigma, \pi, \delta, \dots$  symmetries was sufficient to reach convergence. The total number of states used for time-propagation are limited by an energy cut-off parameter which has been chosen between 10 a.u. and 20 a.u. in order to yield converged results. This resulted in about 17,000, 22,000, and 22,000 states in the calculations for  $\text{N}_2$ ,  $\text{O}_2$ , and  $\text{CO}_2$ , respectively.

The time profile of the applied linearly polarized laser pulse is represented by a  $\cos^2$  vector potential and has in all cases shown a wavelength of 800 nm and a duration of 40 fs. While only results for the experimental peak intensities are shown, a number of calculations for lower peak intensities were performed and no qualitative changes were found for the total ion yields. Thus focal-volume averaging should not influence the main findings of this work, except one case as is discussed below. At the end of the time-propagation calculations (performed in length gauge) the ionization yield is obtained from a sum over the populations of the discretized continuum states. In the case of  $\text{H}_2$  it was demonstrated by a comparison to full two-electron calculations that for ionization yields not exceeding about 10 % the SAE-TDSE results should be multiplied by a factor of 2 in order to account for the two equivalent electrons [9]. Correspondingly, the ionization yields obtained for a given initial orbital were multiplied with the occupation number and orbital degeneracy was explicitly considered. The total ionization is obtained by an incoherent sum of these weighted orbital yields. For the experimental parameters of [6] used in this work this sum remains well below 10 %, except for  $\text{O}_2$  where the maxima almost reach 10 %. Since for  $\text{O}_2$  the contributions from orbitals other than the HOMO are found to be negligible, this does, however, not change

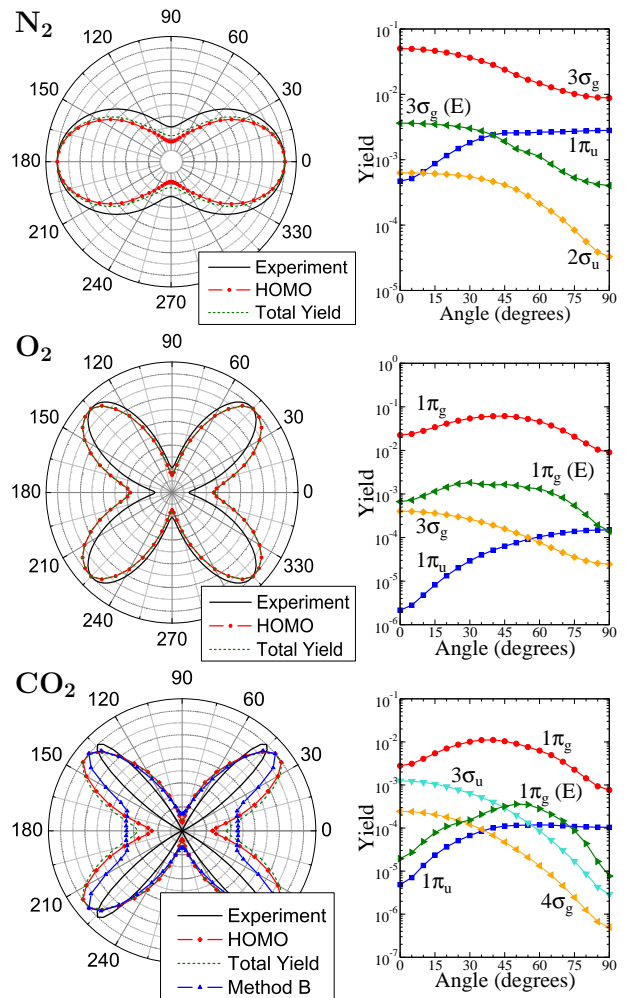


FIG. 1: (Color online) **Left panels:** Normalized ionization yields as a function of the angle between the electric field and the molecular axis: experimental data (black, [6]) and theoretical results (method A) for the HOMO (red dots) and for the total yield (green dashed line). For  $\text{CO}_2$  also the result of method B is shown. **Right Panels:** Ionization yields of the HOMO and some lower lying orbitals (HOMO-X) as well as the excitation yield (E) from the HOMO. **Laser peak intensities:**  $\text{N}_2$  ( $1.5 \times 10^{14}$  W/cm $^2$ ),  $\text{O}_2$  ( $1.3 \times 10^{14}$  W/cm $^2$ ) and  $\text{CO}_2$  ( $1.1 \times 10^{14}$  W/cm $^2$ ).

any of the conclusions of the present work.

Figure 1 shows a comparison of the orientation dependence of the ionization yield of  $\text{N}_2$  obtained in this work (method A) with the experimental data in [6]. Already the pure HOMO ( $3\sigma_g$ ) contribution agrees quite well with experiment, and this agreement is slightly improved, if the contributions of all orbitals are included. As the angle between molecular axis and field vector approaches  $90^\circ$ , there is an increasing contribution from the HOMO-1 ( $1\pi_u$ ). Its inclusion changes the ratio of parallel to perpendicular ionization from 5.7 to 4.4 which then is in reasonable agreement to the experimentally

found  $3.3 \pm 0.4$  [6]. This confirms the importance of the HOMO-1 especially for perpendicular orientation, also found recently for high harmonic generation in [11]. The contribution of the HOMO-2 ( $2\sigma_u$ ) is on the other hand practically negligible, though at  $0^\circ$  it is larger than the one of the HOMO-1.

For  $\text{O}_2$  the agreement between SAE-TDSE and experiment is again good, as is seen from Fig. 1. The small shift of the maxima towards the horizontal axis may be explained by the influence of vibrational motion, since  $\text{O}_2$  should preferentially ionize at smaller internuclear separations than at the equilibrium one [12]. The larger asymmetry between parallel and perpendicular orientation found in the SAE-TDSE is a consequence of the fact that both electrons in the degenerate  $\pi_g$  orbitals ( $\pi_g^x, \pi_g^y$ ) contribute equally in parallel orientation, but effectively only the  $\pi_g^x$  electron contributes in  $x$  direction. The symmetry observed in the experiment is thus somewhat surprising and it may be worthwhile to check the experimental deconvolution procedure in this respect. In fact, an even better agreement is found for all three considered molecules  $\text{N}_2$ ,  $\text{O}_2$ , and  $\text{CO}_2$ , if the contributions from the  $\pi^y$  orbitals are omitted. Compared with  $\text{N}_2$ , the alignment dependence of the ionization yield from the  $\text{O}_2$  HOMO with its  $\pi_g$  symmetry differs clearly, in accordance with expectations based on the corresponding (momentum) densities (see, e.g., Figs. 2 and 3 in [13]). The contributions from the HOMO-1 ( $3\sigma_g$ ) and HOMO-2 ( $1\pi_u$ ) are found to be practically negligible, but their orbital structure is again imprinted in their ionization yields. For parallel alignment the  $3\sigma_g$  orbital of  $\text{O}_2$  is, e.g., much more likely to ionize than for perpendicular alignment and it shows a very similar behavior as the HOMO  $3\sigma_g$  of  $\text{N}_2$ . The same analogy applies for the  $1\pi_u$  orbitals of  $\text{O}_2$  and  $\text{N}_2$ . The found correspondence between orbital structure and ionization behavior for HOMO and HOMO-1 of  $\text{N}_2$  contradicts results of a recent all-electron time-dependent density-functional-theory calculation [14]. Noteworthy, the present SAE-TDSE results for both  $\text{N}_2$  and  $\text{O}_2$  agree better to experiment than the results in [14].

A similar correlation with the orbital shape is found for the orientation dependence of the HOMO and the HOMO- $X$  ( $X=1, 2, 3$ ) of  $\text{CO}_2$ . Although the HOMO of  $\text{O}_2$  and  $\text{CO}_2$  are both  $1\pi_g$  orbitals, the one of  $\text{CO}_2$  is more stretched along the nuclear axis which leads to a more asymmetric orientation dependence (peaking at about  $40^\circ$ ). In that sense the present SAE-TDSE results confirm the conjecture that the alignment dependence of the strong-field ionization reflects the symmetry of the orbital. A prerequisite for this correspondence is the absence of intermediate resonances. The excitation yields to all electronically excited bound states are also shown in Fig. 1. For all three molecules they are much smaller than the ionization yield and, more importantly, follow in shape quite well the angular dependence of the HOMO

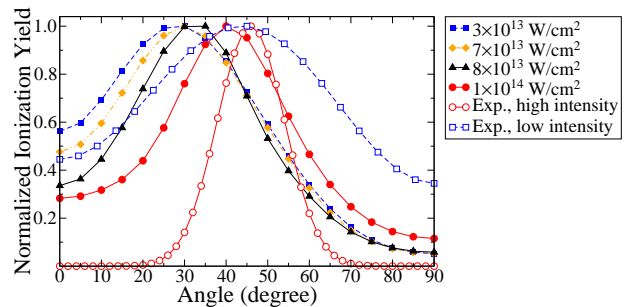


FIG. 2: (Color online) Normalized ionization yield from the HOMO of  $\text{CO}_2$  (method B) for different laser peak intensities between  $3 \times 10^{13} \text{ W/cm}^2$  (as in the experiment [18]) and  $1.1 \times 10^{14} \text{ W/cm}^2$  (experiment in [6]).

ionization yields. Therefore, though excitation may not necessarily be negligible in absolute magnitude for the three considered molecules and laser parameters, it does not modify the orientation dependence of the ion yields.

Nevertheless, the agreement of the  $\text{CO}_2$  result with experiment is not good. The latter found very sharp maxima, the first peaking at about  $46^\circ$ , and extremely small ionization in parallel and perpendicular orientation. Since the contribution from the HOMO-2 ( $3\sigma_u$ ) is non-negligible for the parallel orientation according to SAE-TDSE (in agreement with recent experimental evidence [15]), the agreement gets even worse for the total ionization. Note, however, that the present results agree reasonably well with the measured angular distribution of fragments of  $\text{CO}_2$  in [16]. Furthermore, already in [6] the experimental  $\text{CO}_2$  distribution was found to be disagreeing to simplified SAE models like MO-ADK and MO-SFA. Since the present SAE-TDSE is a stringent test of the SAE beyond such simplified models, it might be concluded that the deviation to experiment is a breakdown of the SAE itself, if it is not experimentally caused as is proposed in a recent compilation of theoretical results [17]. The most likely explanation for the observed sharp angular distribution appears to be an intermediate resonance whose position is either badly or (in the case of doubly-excited states) not at all predicted within SAE. Clearly, an experimental wavelength (or intensity) scan should reveal such a resonance and would thus be very desirable. In fact, there exists one further experimental investigation of the orientation dependent ionization of  $\text{CO}_2$ . In [18] data are presented for an about 3 to 4 times lower peak intensity than in [6]. The distribution is much broader and thus in better agreement with simplified models.

So far, all discussed results were obtained with method A. While there is no qualitative change when applying method B to  $\text{N}_2$  and  $\text{O}_2$ , this is not the case for  $\text{CO}_2$  (see Fig. 1). In this case the SAE-TDSE results are more similar to the experiment, since the peak shifts towards

a larger angle and becomes narrower. Figure 2 shows the results obtained with method B for different laser intensities and reveals an even more interesting effect. The peak widths become pronouncedly narrower with increasing intensity. This is in accordance with the experimental results of [6] and [18]. In fact, there is a pronounced change occurring at a peak intensity around  $8 \times 10^{13}$  W/cm<sup>2</sup> and thus in between the two experimentally investigated intensities. A more detailed analysis reveals that this effect is due to a field-induced coupling between the field-free HOMO ( $1\pi_g$ ) and the HOMO-1 ( $1\pi_u$ ). In fact, at an intensity of about  $8 \times 10^{13}$  W/cm<sup>2</sup> the different ac Stark shifts of the two involved orbitals allow strong Rabi oscillations to occur and the resulting coherent trapping of the electron reduces the ionization probability.

Due to symmetry, the  $1\pi_g$  HOMO and the  $1\pi_u$  HOMO-1 are coupled by a field parallel to the molecular axis. Therefore, the effective intensity responsible for a coupling of these states is the component parallel to the molecular axis. For a given intensity the transition may be resonant for the parallel orientation, but is not yet resonant for other orientations. A further increase of the intensity allows then a larger range of orientations to become resonant. As a consequence, the orientational distribution becomes narrower, as the ionization probability decreases for an increasing range of angles close to 0° (or 180°). It was confirmed that the shift of the maximum of the yield agrees with the corresponding shift of the projection of the laser field onto the molecular axis.

Note, there are two effects of the strong field that lead to coherent core trapping. First, the Stark shift brings the orbitals into resonance. (Note, however, that for N<sub>2</sub> the ac Stark shift suppresses the one-photon coupling between HOMO and HOMO-1 that in the field-free situation would be almost resonant for 800 nm photons.) Second, the field-induced quiver motion temporarily depletes the *field-free* core orbital. Clearly, the present theoretical results alone would not be conclusive. Although the adopted approximation of an independent response of the electrons should be reasonable for intense fields (cf. [9]), the results cannot be expected to be quantitatively correct. In fact, due to the intensity dependence also focal-volume effects are relevant. However, together with the experimental findings the present results strongly suggest that coherent core trapping is responsible for the unexpected experimental results observed for CO<sub>2</sub>. The field-free excited states (and their population) are on the other hand not found to lead to substantial effects for the considered examples, in contrast to the interpretation given in [19].

In summary, we have reproduced satisfactorily existing experimental data for the angle-resolved ionization of the diatomic molecules N<sub>2</sub> and O<sub>2</sub> in intense short laser pulses. This shows the potential of the present SAE-TDSE approach that had so far only been tested for H<sub>2</sub>. These results support the principle idea of orbital map-

ping, but we also observe important contributions from the HOMO-X that may distort the tomographical picture of the HOMO as in N<sub>2</sub>. On the other hand, CO<sub>2</sub> is an example for an intensity-dependent breakdown of the orbital tomography that appears to be caused by a field-induced coupling of the HOMO with the core. This may explain why two experiments performed with different laser intensities observed different angular ionization patterns.

The authors would like to thank D. Pavičić and I. Thomann for kindly providing the experimental data and COST *CM0702* for financial support. SP, YV, and AS acknowledge financial support from the *Stifterverband für die Deutsche Wissenschaft*, the *Fonds der Chemischen Industrie*, and *Deutsche Forschungsgemeinschaft* (SFB 450/C6 and Sa936/2), AC within SFB 658, and PD by CNR-INFM Democritos and INSTM Crimson.

- 
- [1] E. Goll, G. Wunner, and A. Saenz, *Phys. Rev. Lett.* **97**, 103003 (2006).
  - [2] T. Ergler, B. Feuerstein, A. Rudenko, K. Zrost, C. D. Schröter, R. Moshhammer, and J. Ullrich, *Phys. Rev. Lett.* **97**, 103004 (2006).
  - [3] S. Baker, J. S. Robinson, C. A. Haworth, H. Teng, R. A. Smith, C. C. Chirilă, M. Lein, J. W. G. Tisch, and J. P. Marangos, *Science* **312**, 424 (2006).
  - [4] J. Itatani, J. Levesque, D. Zeidler, H. Niikura, H. Pépin, J. C. Kieffer, P. B. Corkum, and D. M. Villeneuve, *Nature* **432**, 867 (2004).
  - [5] M. Meckel, D. Comtois, D. Zeidler, A. Staudte, D. Pavičić, H. C. Bandulet, H. Pépin, J. C. Kieffer, R. Dörner, D. M. Villeneuve, et al., *Science* **320**, 1478 (2008).
  - [6] D. Pavičić, K. F. Lee, D. M. Rayner, P. B. Corkum, and D. M. Villeneuve, *Phys. Rev. Lett.* **98**, 243001 (2007).
  - [7] X. M. Tong, Z. X. Zhao, and C. D. Lin, *Phys. Rev. A* **66**, 033402 (2002).
  - [8] J. Muth-Böhm, A. Becker, and F. H. M. Faisal, *Phys. Rev. Lett.* **85**, 2280 (2000).
  - [9] M. Awasthi, Y. V. Vanne, A. Saenz, A. Castro, and P. Decleva, *Phys. Rev. A* **77**, 063403 (2008).
  - [10] R. van Leeuwen and E. J. Baerends, *Phys. Rev. A* **49**, 2421 (1994).
  - [11] B. K. McFarland, J. P. Farrell, P. H. Bucksbaum, and M. Gühr, *Science* **322**, 1232 (2008).
  - [12] A. Saenz, *J. Phys. B* **33**, 4365 (2000).
  - [13] D. B. Milošević, *Phys. Rev. A* **74**, 063404 (2006).
  - [14] D. A. Telnov and S.-I. Chu, *Phys. Rev. A* **79**, 041401 (2009).
  - [15] O. Smirnova, Y. Mairesse, S. Patchkovskii, N. Dudovich, D. Villeneuve, P. Corkum, and M. Y. Ivanov, *Nature* **460**, 972 (2009).
  - [16] A. Alnaser, C. Mahajan, X. Tong, B. Ulrich, P. Ranitovic, B. Shan, Z. Chang, C. Lin, C. Cocke, and I. Litvinyuk, *Phys. Rev. A* **71**, 031403(R) (2005).
  - [17] S.-F. Zhao, C. Jin, A.-T. Le, T. F. Jiang, and C. D. Lin, *Phys. Rev. A* **80**, 051402 (2009).
  - [18] I. Thomann, R. Lock, V. Sharma, E. Gagnon, S. T.

- Pratt, H. C. Kapteyn, M. M. Murnane, and W. Li, J. Phys. Chem. A **112**, 9382 (2008). 023401 (2009).
- [19] M. Abu-samha and L. B. Madsen, Phys. Rev. A **80**,